SDC-91-154

SDC
SOLENOIDAL DETECTOR NOTES

MUON SYSTEM ALIGNMENT STUDIES

October 30, 1991

Jim Wiss
University of Illinois

Jim Wiss

~~November 26,~~ Oct 30, 1991

Muon System Alignment Studies

This note reports on studies of the effects of muon chamber misalignment on the momentum resolution and muon matching obtainable for several off line and 2nd level trigger muon scenarios. We hope such studies can serve to set alignment criteria on the components of the muon system. Presumably the off line criteria set tolerances on the *knowledge* of muon chamber misalignment as opposed to trigger criteria which set tolerances on the *placement* of muon chamber components. This memo augments the work described in the July 31, 1991 memo *Alignment Resolution Studies of the Muon System* by Jim Wiss. The previous memo concentrated on the question of how Gaussian distributed chamber station misalignments degrade momentum resolution. This work concentrates on the momentum biases created by rigid body chamber station misalignment. We begin by describing the technique, and then show results.

1. Technique

In a linearized fit, changes in the track parameters (t_α) are just a linear function of changes in the measured coordinates (w_i). We will call the linear transformation the ρ matrix. Systematic residuals in the coordinates created by chamber misalignment will create average biases in track parameters given by:

$$< \Delta t_\alpha >= \rho_{\alpha i} \ < \Delta w_i > \qquad 1$$

The calculation of alignment biases involves both the ρ matrix and the dependence of $< \Delta w_i >$ on the misalignment parameters. We begin with a discussion of the ρ matrix.

The $\rho_{\alpha i}$ matrix element serves as a direct measurement of the importance of the information of the i'th coordinate in determining the α'th track parameter. The ρ matrix depends on the coordinate covariance matrix assumed in performing

the fit C_{ij} as well as the transport matrix which ($T_{i\alpha}$) which relates the predicted coordinate from the track parameters ($w_i = T_{i\alpha} t_\alpha$):

$$\rho_{\alpha i} = H^{-1}_{\alpha\beta}\ C^{-1}_{ij}\ T_{j\beta} \quad \text{where} \quad H_{\alpha\beta} = C^{-1}_{ij}\ T_{i\alpha}\ T_{j\beta}$$

To get the best (minimal variance) results, the coordinate covariance matrix should reflect multiple scattering as well as measurement errors.

Figure 1 shows ρ matrix elements for the two θ and the two ϕ layers placed in BW1 as a function of P_t for muons created at $\eta = 0$. The ρ matrix is for a fit where information from the beam constraint ($\sigma = 20\mu$), silicon , CTD , and BW1 $\rightarrow$ BW3 is combined to find the track curvature. The ρ matrix depends significantly on η. We consider a muon layout with two θ planes in each of the three muon stations and two ϕ layers placed in just BW1. The rapid growth in ρ with increasing P_t for the two ϕ layers shows that they play an active role in determining momentum even at modest P_t. The growth in the ρ elements for the two θ layers is considerably more gradual. Evidently the muon toroid acts as a significant source curvature information only at large P_t.

We note that at low P_t the ρ elements for the inner and outer ϕ planes have the opposite signs. This means that the curvature fit is using the ϕ coordinate differences or essentially using the ϕ slope in BW1. Rigid body misalignment of the whole BW1 station will create nearly equal displacements in the two ϕ layers and thus a canceling momentum bias in the low P_t limit. At larger P_t, the ρ elements for the two ϕ layers have the same sign and rigid body misalignment becomes more important. Evidently in the high P_t domain the fit is concentrating on the the ϕ intercept rather than the ϕ slope. In the 1 TeV P_t domain, the θ layers become as important as the ϕ layers in BW1 in determining track curvature.

We next address the calculation of the chamber plane residuals (Δw_i) induced by rigid body misalignment error. The barrel muon system consists of a series of detector planes which can be specified by a read-out direction ($\hat{w}$), a plane

normal ($\hat{\eta}$), and an arbitrary point in the plane ($\vec{D}$). The below table gives a set of these vectors for two types of projections at radius R. The $\hat{y}$ geometry serves as a non-projective ϕ geometry for the first octant (the octant normal to $\phi = 0$). In the projective θ geometry, each plane (drift cell) is orientated such that its normal points back to the origin.

Table 1 – Detector Geometries in $\phi \approx 0$ Octant

Geometry	$\vec{D}$	$\hat{\eta}$	$\hat{w}$
$\hat{y}$	$(R \quad 0 \quad 0)$	$(1 \quad 0 \quad 0)$	$(0 \quad 1 \quad 0)$
projective θ	$(R \quad 0 \quad R/T_\theta)$	$(S_\theta \quad 0 \quad C_\theta)$	$(-C_\theta \quad 0 \quad S_\theta)$

Where $S_\theta \equiv sin\ \theta$, $C_\theta \equiv cos\ \theta$, $T_\theta \equiv tan\ \theta$

Let us imagine a track which passes through a point $\vec{M}$ and travels in a direction $\hat{p}$. The intersection ($\vec{x}$) of the track with the detector plane is given by:

$$\vec{x} = \vec{M} + \frac{\ell \hat{p}}{\hat{p} \cdot \hat{\eta}} \quad \text{where} \quad \ell = \hat{\eta} \cdot \left(\vec{D} - \vec{M}\right) \qquad 2$$

When viewed relative to a chamber station, a shift misalignment ($\vec{\Delta}$) can represented as a change in $\Delta\vec{M} = -\vec{\Delta}$ of the track origin and an angular misalignment can be a rotation ($\vec{\alpha}$) of $\hat{p} = -\vec{\alpha} \times \hat{p}$. The misalignment will create a change in coordinates given by:

$$\Delta w = -\hat{w}_i \frac{\partial \vec{x}_i}{\partial \vec{M}_j} \vec{\Delta} - \hat{w}_i \frac{\partial \vec{x}_i}{\partial \hat{p}_j} (\vec{\alpha} \times \hat{p})_j \qquad 3$$

The partial derivatives of Eqn. (2) are:

$$\frac{\partial \vec{x}_i}{\partial \vec{M}_j} = \delta_{ij} - \frac{\hat{p}_i \hat{\eta}_j}{\hat{p} \cdot \hat{\eta}} \quad ; \quad \frac{\partial \vec{x}_i}{\partial \hat{p}_j} = \frac{\ell}{\hat{p} \cdot \hat{\eta}} \left(\delta_{ij} - \frac{\hat{p}_i \hat{\eta}_j}{\hat{p} \cdot \hat{\eta}}\right) \qquad 4$$

Combining Eqn. (3) and (4) we have:

$$\Delta w = -\vec{g} \cdot \vec{\Delta} - \frac{\ell}{\hat{p} \cdot \hat{\eta}} \vec{g} \cdot \vec{\alpha} \times \hat{p} \quad \text{where} \quad \vec{g} = \hat{w} - \frac{\hat{\eta}\ \hat{p} \cdot \hat{w}}{\hat{p} \cdot \hat{\eta}} \qquad 5$$

Figure 2-4 show the residuals versus ϕ resulting from a 0.5 mm x shift (Figure

2) , a pitch rotation of 0.1 mrad about the $\hat{x}$ axis (Figure 3), and a roll of 0.1 mrad about the $\hat{z}$ axis. The solid curves are for Δw_ϕ ; the dashed curves are for Δw_θ. The figures are for muons produced at $\eta = 1.5$ (or $\theta = 25.2^o$). The residuals are computed using Eqn. (5), where $\hat{p} = (\, C_\phi S_\theta \quad S_\phi S_\theta \quad C_\theta \,)$, and $\vec{D}$, $\hat{\eta}$, and $\hat{w}$ are taken from Table 1.

Several features are apparent from inspection of Figures 2-4. The residual pattern for (transverse) shifts and rotations are roughly sinusoidal with the Δw_ϕ being 90° out of phase with the Δw_θ phase. Significant discontinuities are present which reflect the octant structure of the muon chambers. The curved sections are essentially due to the same effects which create the ϕ angular factors described in my September 23, 1991 memo, *Octagonal Geometry Effects*. At $\eta = 0$, the transverse shifts create Δw_ϕ residuals but no Δw_θ residuals. The Δw_θ residuals grow from zero as η increases. This pattern is reversed for the case of transverse rotations (pitch and yaws). The approximate amplitude and phase of the various misalignments follows from simple trigonometric arguments and is summarized in Table 2.

Table 2 : Residual Envelope Functions

	MisAlign amount	Δw_ϕ	Δw_θ
Shift$_\perp$	$(\, \Delta_\perp cos\phi_s \quad \Delta_\perp sin\phi_s \,)$	$\Delta_\perp \; sin\;(\phi - \phi_s)$	$\Delta_\perp \; cos\theta \; cos(\phi - \phi_s)$
Shift$_z$	Δ_z	0	$-\Delta_z \; sin\theta$
Rot$_\perp$	$(\, \alpha_\perp cos\phi_r \quad \alpha_\perp \; sin\phi_r \,)$	$\alpha_\perp \; R \; cos(\phi - \phi_r)/tan\;\theta$	$-\alpha_\perp \; R \; sin(\phi - \phi_r)/sin\;\theta$
Roll	α_z	$R\;\alpha_z$	$-R\;\alpha_z \; cos\;\theta \;\; sin\;(\phi - \phi_{\rm oct})$

$\phi - \phi_{\rm oct}$ is the angle of the track wrt the octant normal

2. Results

In this section we develop alignment tolerances for rigid body motions of BW1 for a variety of curvature fits. We are guided by selecting misalignment tolerances which insure that P_t biases are always less than some fraction of the

P_t resolution up to some desired P_t over all ϕ and the η covered by the barrel muon system. The criteria can be computed using the calculations summarized in Tables 3 - 6. Throughout these calculations we assume a "minimal" muon chamber layout with two projective θ layers in BW1 $\rightarrow$ BW3 and two ϕ layers in BW1 only. The radial geometry is summarized below:

Table 3 : Radial Geometry

	R_{in}	R_{out}
Calorimeter	2.1 m	4.32 m
BW1	5.67	6.27
Toroid	6.45	7.95
BW2	8.18	8.53
BW3	9.78	10.66

(a) Full system fits

We begin by illustrating the effects of rigid body misalignment on BW1 in a curvature fit using the complete SDC detector (beam constraint, silicon , CTD, and muon system). Figure 5 shows the error normalized momentum bias ($\Delta P_t/\sigma P_t$) as a function of P_t for the case of $\eta = 0$, $\phi = 0$ muons for various misalignment errors (a 0.5 mm $\hat{y}$ shift , 0.5 mm $\hat{z}$ shift , a 0.1 mrad yaw , and a 0.1 mrad roll). The orientation of the shifts was chosen to give a maximum bias (for $\eta = 0$ muons) at $\phi = 0$. The magnitude of the misalignments were chosen to give a roughly $\pm 1\sigma$ bias at $P_t = 2\ TeV$, $\eta = 0$. Figure 5 shows that misalignments which primarily affect Δw_ϕ are far more important than misalignments which primarily affect Δw_θ in the domain $P_t < 200\ GeV$. The relative importance of ϕ layers rather than θ layers at low P_t is demonstrated by the strength of their respective ρ matrix elements shown in Figure 1.

Figure 6 shows the maximum $\Delta P_t/\sigma P_t$ as a function of ϕ for $P_t = 2000\ GeV$ muons for transverse and longitudinal shifts and rotations. For transverse shifts

and all rotations the maximum misalignment effect occurs the largest η (drawn for $eta = 1.5$); for $\hat{z}$ shifts the curve is drawn for $\eta = 0$ where the effect of a $\hat{z}$ shift creates maximum bias. Much of the ϕ residual structure seen in Figures 2 - 4 is recognizable in the ϕ bias structure shown in Figure 6. For $P_t = 2000\ GeV$, $\eta =$ 1.5 muons, both Δw_ϕ and Δw_θ residuals play important roles and phases other than 0 and 90°'s are observed in the transverse shifts and rotations. The effects of shifts and rolls (rotations about $\hat{z}$) are well balanced; the effects of transverse rotations (pitches and yaws) is more important by a factor of ≈ 3. Much of the increased bias created by pitch and yaw relative to shifts and rolls is due to the aspect ratio of the barrel detector (it is about 2.12 times longer than its radius if it extended out to $\eta = 1.5$). The below table gives both the maximum and ϕ averaged rms values of $\Delta P_t/\sigma P_t$ for the case of $P_t = 2\ TeV$ muons. We also summarize calculations for misalignments in BW2 and BW3. Recall that in these calculations BW1 is the only muon station which contains ϕ layers.

Table 4 – Full system :B.C. , Si , CTD , & Muon System
Maximum & RMS Deviations at $P_t = 2\ TeV$

	BW1	BW1	BW2	BW2	BW3	BW3
	max	rms	max	rms	max	rms
.5 mm shift x	1.19	0.79	0.61	0.43	0.98	0.69
.5 mm shift z	0.91	0.91	0.48	0.48	0.86	0.86
.1 mrad pitch	3.60	2.34	2.59	1.82	5.20	3.65
.1 mrad roll	1.09	0.64	0.39	0.23	0.79	0.45

The momentum biases simply scale with the magnitude of the misalignments. One can simply scale the indicated misalignment in column one by the ratio of the desired error normalized tolerance to the maximum or RMS computed bias to set alignment tolerances. If we wished to limit biases to less than 1 σ over the full $\eta - \phi$ range at 2 TeV P_t, shifts will have to be kept to less than ≈ 0.5 mm , rolls will have to be kept to ≈ 0.1 mrad and pitches and yaws will have

to be kept to ≈ 27 μrad of BW1 relative to the CTD. These tolerances mean that all corners of the barrel muon detector should be located to within ≈ 0.5 mm relative to the CTD insure good performance over the full detector up to 2 TeV. These conclusions are consistent with those reached in my earlier memo *Alignment Resolution Studies of the Muon System.*

(b) Hi Luminosity option

We next consider curvature measurement in the high luminosity limit where the CTD has too high an occupancy to be useful. In the high luminosity fit, the curvature is measured using information from the beam constraint, silicon, and muon system. Figure 7 shows the momentum bias divided by the momentum error ($\Delta P_t/\sigma P_t$) as a function of P_t for the case of $\eta = 0$, $\phi = 0$ muons for various misalignment errors (a 0.5 mm $\hat{y}$ shift , 0.5 mm $\hat{z}$ shift , a 0.1 mrad yaw , and a 0.1 mrad roll). We see that the misalignments which most affect w_θ ($\hat{z}$ shift and yaw) are about a factor of 4 less important relative to the misalignments which primarily affect w_θ. This is in contrast to the results of Figure 5 for the full muon fit and reflects the much smaller size of the sum of the θ plane ρ matrix elements in this type of fit for muons produced at $\eta = 0$.

Figure 8 shows the maximum $\Delta P_t/\sigma P_t$ as a function of ϕ for $P_t = 2000\ GeV$ muons for transverse and longitudinal shifts and rotations. For transverse shifts and all rotations the maximum misalignment effect occurs the largest η (drawn for $\eta = 1.5$). For $\hat{z}$ shifts the curve is drawn for $\eta = 0$ where the effect of a $\hat{z}$ shift creates maximum bias. Table 5 gives the maximum and (ϕ averaged) rms error normalized momentum biases for misalignments in BW1 $\rightarrow$ BW3.

Table 5 – High Lum Option: B.C. , Si & Muon System only
Maximum & RMS Deviations at $P_t = 2\ TeV$

	BW1	BW1	BW2	BW2	BW3	BW3
	max	rms	max	rms	max	rms
.5 mm shift x	1.03	0.61	1.09	0.77	0.61	0.43
.5 mm shift z	0.25	0.25	0.56	0.56	0.31	0.31
.1 mrad pitch	2.79	1.67	4.65	3.26	3.26	2.29
.1 mrad roll	1.22	0.90	0.70	0.41	0.49	0.28

We see from Table 5, that the shift z alignment tolerances can be relaxed to about 1 mm for the high luminosity fits. Transverse misalignment must be kept to within ≈ 0.5 mm.

(c) Muon Toroid as a Stand Alone System

By a stand along system, we mean that the muon system provides momentum measurement by measuring the θ bend through the 1.5 m toroid without any help from the beam constraint, CTD , or silicon. One can imagine the stand alone use of muon system as a second level muon trigger as well as an off line tool which provides a redundant momentum measurement of muons for the purpose of matching and punch through rejection. For triggering purposes a $P_t = 100\ GeV$ seems appropriate, for off line purposes the 2 TeV scale may be relevant. Figure 9 and 10 show error normalized biases for BW1 misalignments subject to our standard misalignments ((a 0.5 mm $\hat{y}$ shift , 0.5 mm $\hat{z}$ shift , a 0.1 mrad pitch , and a 0.1 mrad roll) for $P_t = 2\ TeV$ (Figure 9) and $P_t = 100\ GeV$ (Figure 10). Table 6 & 7 give the error normalized maximum and rms biases over the range ($0 < |\eta| < 1.5$ for misalignments in BW1 $\rightarrow$ BW3.

Table 6 – Toroid Stand Alone

Maximum & RMS Deviations at $P_t = 2\ TeV$

	BW1	BW1	BW2	BW2	BW3	BW3
	max	rms	max	rms	max	rms
.5 mm shift x	0.81	0.57	1.83	1.29	1.02	0.72
.5 mm shift z	0.90	0.90	2.04	2.04	1.14	1.14
.1 mrad pitch	2.35	1.65	7.83	5.49	5.47	3.84
.1 mrad roll	0.36	0.21	1.18	0.68	0.83	0.48

Table 7 – Toroid Stand Alone

Maximum & RMS Deviations at $P_t = 100\ GeV$

	BW1	BW1	BW2	BW2	BW3	BW3
	max	rms	max	rms	max	rms
.5 mm shift x	0.08	0.06	0.23	0.16	0.15	0.11
.5 mm shift z	0.18	0.18	0.44	0.44	0.27	0.27
.1 mrad pitch	0.18	0.13	0.98	0.69	0.80	0.56
.1 mrad roll	0.03	0.02	0.15	0.09	0.12	0.07

The results of Table 7 indicate that the $R\theta$ misalignments of BW2 must be kept below ≈2 mm to keep $\Delta P_t < \sigma P_t$ at $P_t = 100\ GeV$. Since the second level trigger does not have the time to put in alignment corrections, this means that BW2 must really be placed in space within this ≈ 2 mm tolerance. To maintain $\Delta P_t < \sigma P_t$ at $P_t = 2\ TeV$ over the full η range will require $R\theta$ misalignments of less than 0.25 mm. This is a tolerance on the knowledge of the BW2 position. As one would expect, the roll tolerances in this type of fit are rather loose.

(d) ϕ Second Level Trigger

Next we discuss studies of the alignment tolerance for a ϕ second level trigger where information from a beam constraint, the outermost two layers of the CTD

(providing an angular resolution of ≈2 mrad) is combined with information from the two ϕ layers in BW1 to measure momenta. No use is made of the toroid. The only relevant misalignment is for the ϕ planes in BW1. Figure 11 shows the error normalized biases for our standard list of misalignments (a 0.5 mm $\hat{x}$ shift , 0.5 mm $\hat{z}$ shift , a 0.1 mrad pitch , and a 0.1 mrad roll) for muons with $\eta = 1.5$ & $P_t = 100\ GeV$. The maximum and RMS normalized biases are summarized in Table 8 for $P_t = 50$, 100 & 200 GeV.

Table 8 – ϕ 2nd Level Trigger
Maximum & RMS Deviations for BW1 Motions

	50 GeV	50 GeV	100 GeV	100 GeV	200 GeV	200 GeV
	max	rms	max	rms	max	rms
.5 mm shift x	0.0644	0.0466	0.1057	0.0765	0.1663	0.1203
.5 mm shift z	0.0000	0.0000	0.0000	0.0000	0.0000	0.0000
.1 mrad pitch	0.1067	0.0739	0.2017	0.1397	0.3843	0.2661
.1 mrad roll	0.0543	0.0489	0.1026	0.0924	0.1954	0.1761

Table 8 shows that BW1 alignment tolerances must be kept to 3 mm in the Rϕ direction to keep the maximum biases to less than 1 σ for $P_t = 200\ GeV$ muons in the range $0 < \eta < 1.5$. If one is only interested in maintaining this performance up to $P_t = 100\ GeV$, the alignment tolerance can be relaxed to ≈ 5 mm. Presumably alignment corrections cannot be made at the trigger level and hence BW1 would actually have to be placed relative to the CTD within these tolerances. The tolerances required in the 2nd level ϕ trigger are presumably looser than in the 2nd level θ trigger since the CTD does much of the measurement work in the ϕ trigger.

(e) Muon Matching

Finally we address the effects of chamber misalignment on the ability to match muons with putative tracks measured in the CTD. We assume that the off

line matching of the muon chamber hits with a possible CTD track is performed using a χ^2 test to the extrapolated track trajectory. A track is matched if it has a minimum, acceptable confidence level to the muon chamber hits where the confidence level is chosen so that the vast majority (*eg* 98 %) of real CTD muons are successfully matched (*eg* , $CL > 0.02$). The χ^2 is kept as low as possible (consistent with keeping muon efficiency) to eliminate confusion resulting when an adjacent track has sufficiently similar track parameters that its extrapolation satisfies the muon confidence level cut. A study of matching confusion is presented in the memo *Muon Matching Studies* by Steve Errede , Rob Gardner, and Jim Wiss.

The effects of misalignment will be to create a ϕ dependent average χ^2 increase of which is proportional to the square of the misalignment strength. If the $\Delta\chi^2$ were sufficiently large, real muons would fail to satisfy the matching χ^2 cut resulting in efficiency losses. To get a feel for these effects we compute the χ^2 increase due to misalignments as:

$$\Delta\chi^2 = \Delta\ w_i\ C_{ij}^{-1}\Delta w_j \quad \text{where } \Delta w_i \text{ are due to misalignment}$$

Figure 12 shows $\sqrt{\Delta\chi^2}$ as a function of ϕ for 2 TeV muons for our four standard misalignments. Table 7 & 8 summarize the maximum and RMS $\sqrt{\Delta\chi^2}$ as one scans over ϕ for the case of 2 TeV and 50 GeV muons.

Table 9 – $\sqrt{\Delta\chi^2}$

Maximum & RMS $\sqrt{\Delta\chi^2}$ at $P_t = 2\ TeV$

	BW1	BW1	BW2	BW2	BW3	BW3
	max	rms	max	rms	max	rms
.5 mm shift x	2.27	1.82	2.07	1.46	1.42	1.00
.5 mm shift z	2.55	2.55	2.33	2.33	1.71	1.71
.1 mrad pitch	6.91	5.34	8.89	6.24	7.41	5.20
.1 mrad roll	2.08	1.73	1.35	0.78	1.12	0.65

Table 10 – $\sqrt{\Delta\chi^2}$

Maximum & RMS $\sqrt{\Delta\chi^2}$ at $P_t = 50\ GeV$

	BW1	BW1	BW2	BW2	BW3	BW3
	max	rms	max	rms	max	rms
.5 mm shift x	0.30	0.22	0.65	0.46	0.54	0.38
.5 mm shift z	0.48	0.48	0.82	0.82	0.62	0.62
.1 mrad pitch	0.96	0.68	2.83	1.99	2.45	1.72
.1 mrad roll	0.17	0.12	0.43	0.25	0.37	0.21

Table 9 suggests that the alignment tolerances required to keep $\Delta\chi^2 < 1$ at 2 TeV correspond to $\approx 0.25mm$ position uncertainties. At 50 GeV, the matching alignment criteria can be relaxed by roughly a factor of 3 ($\approx$1 mm position uncertainty).

3. Conclusions

This work has concentrated on setting alignment criteria both for use in possible 2nd level triggers and off line applications including momentum resolution and matching muon tracks in highly clustered jets. We been guided by the concept that momentum biases induced by misalignment should be less than the momentum resolution over the full $\eta - \phi$ range spanned by the barrel muon detector up to some desired momentum. For off line studies we choose a maximum P_t of 2 TeV ; for triggering we typically use a maximum P_t of 100 GeV.

Although each type of misalignment has its own unique pattern of momentum biases within the context of a given curvature fit, a general picture emerges for what we hope are reasonable alignment tolerances. Generally the position tolerances for triggering purposes must be kept within $2 \rightarrow 3$ mm. To maintain performance from $0 < |\eta| < 1.5$, this implies pitch and yaw tolerances of roughly 150 μrad. These are probably tolerances on the actual transverse and longitudinal positions of the muon chamber stations relative to the CTD.

Off line analysis tolerances at $P_t = 2$ TeV range from roughly $0.2 \rightarrow 0.5$ mm. The looser tolerances are for fits which combine information from other trackers such as the CTD or silicon system. The tighter tolerance is for redundant measurement by the muon toroid as a stand alone system or for matching high P_t tracks measured in the CTD to hits in the muon system. These position tolerances imply pitch and yaw tolerances of $< 15\ \mu rad$ if one wishes to maintain performance up to $|\eta| < 1.5$.

Fig 1 -- ρ versus Pt

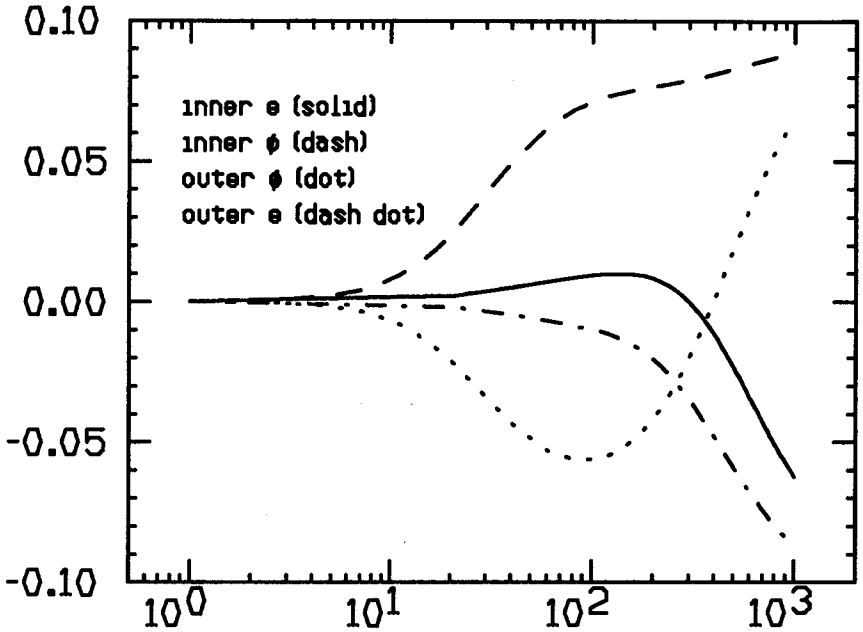

Fig 2 -- Resid vrs ϕ (.5 mm Shiftx)

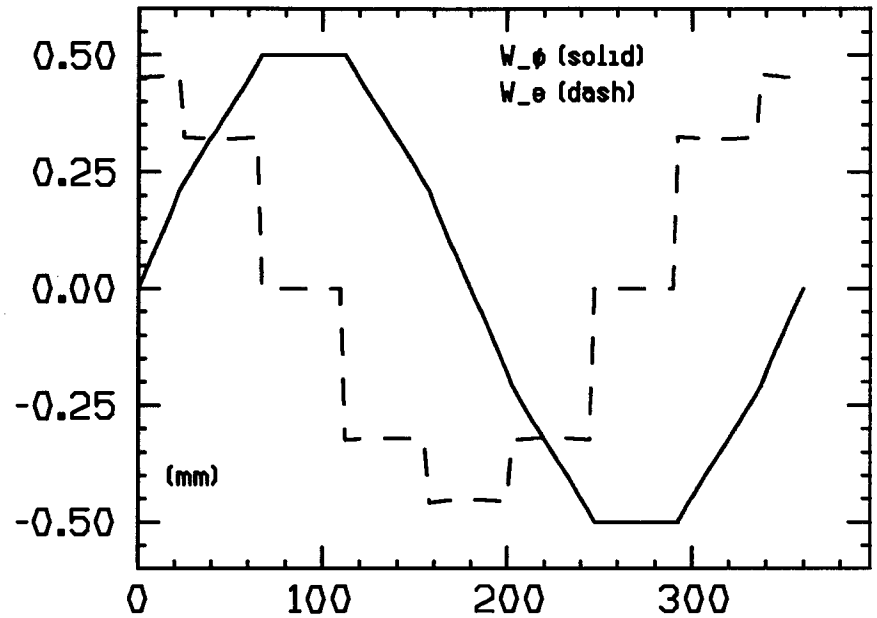

Fig 3 -- Resid vrs ϕ (.1 mrad pitch)

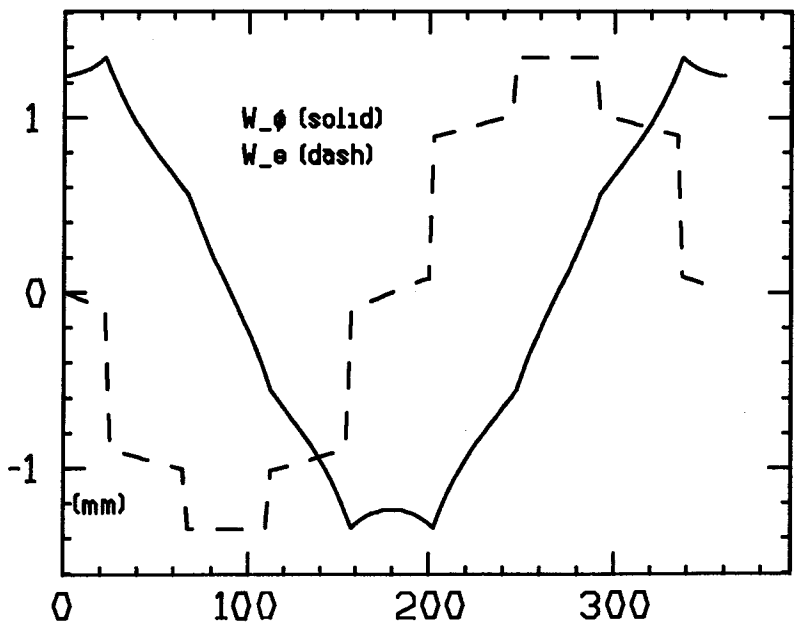

Fig 4 -- Resid vrs ϕ (.1 mrad roll)

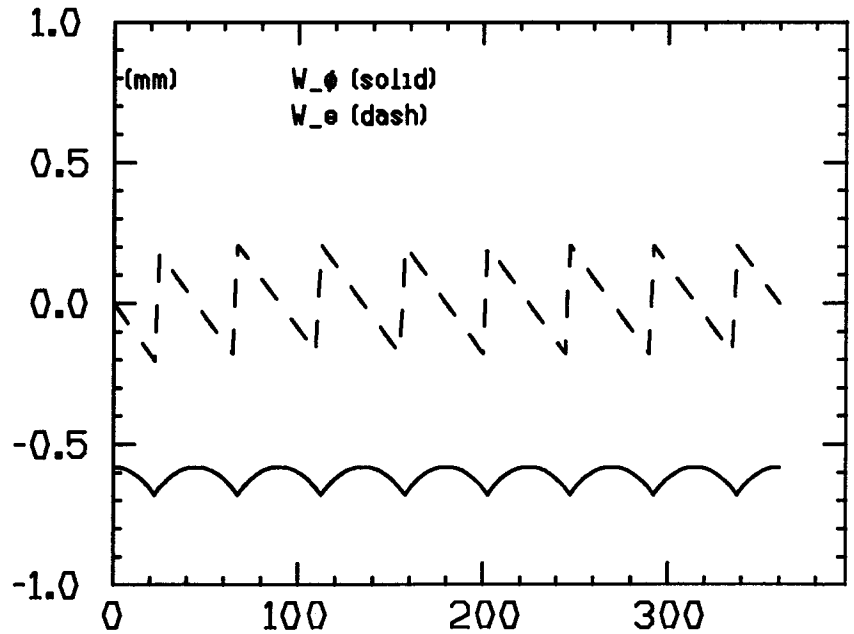

Fig. 5 Δ/σ vrs Pt (BW1)

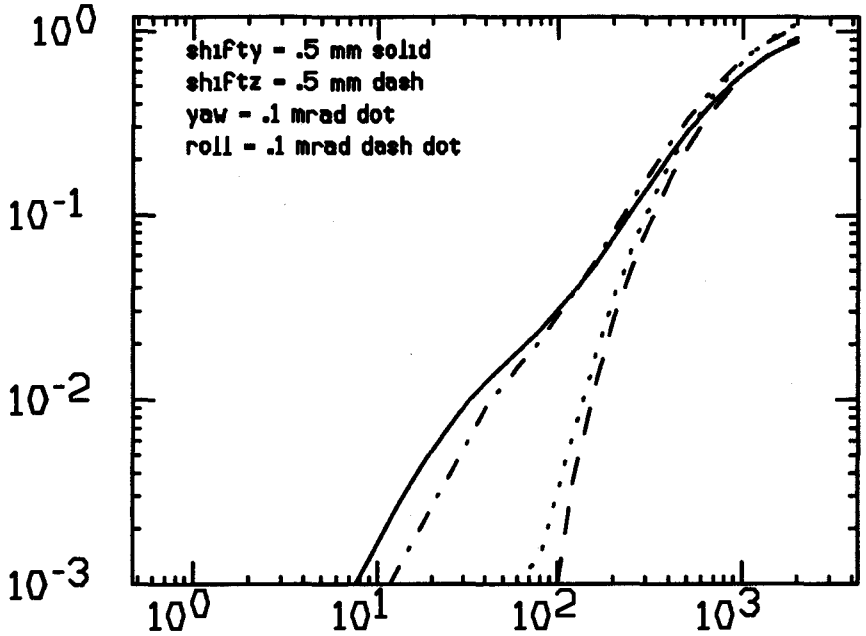

Fig 6 Δ/σ vrs φ (Full Fit BW1)

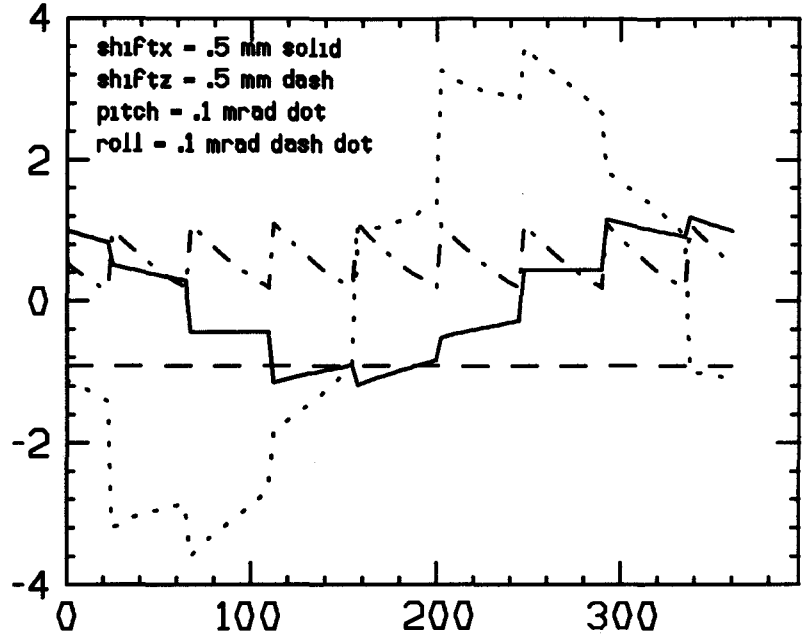

Fig 7 Δ/σ vrs Pt (HI LUM BW1)

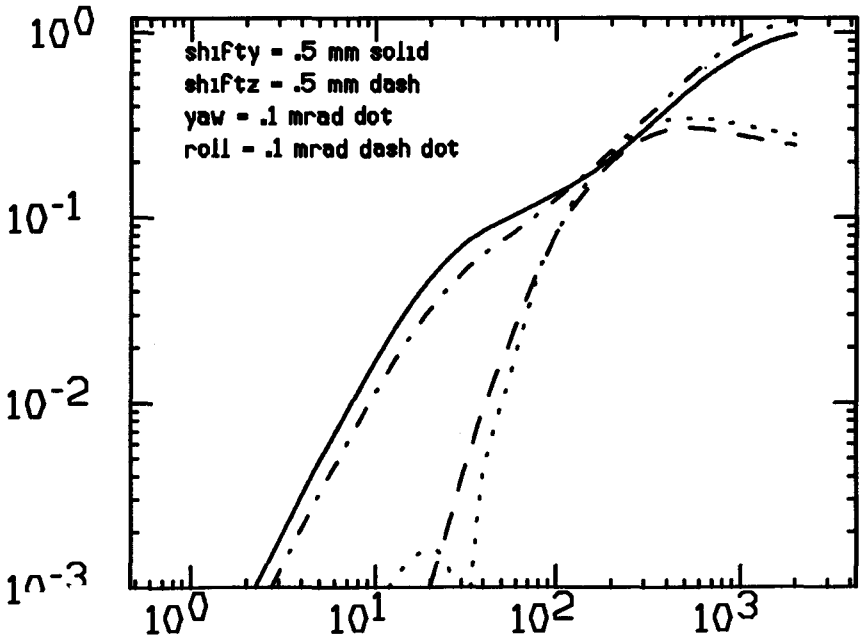

Fig 8 Δ/σ vrs φ (HI LUM BW1)

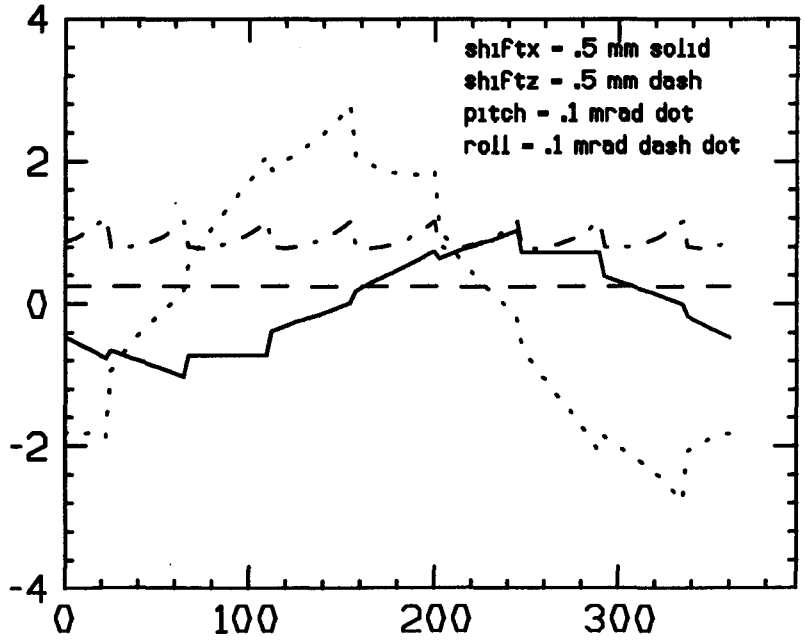

Fig 9 -- Δ/σ vs φ Tor only Pt = 2 TeV

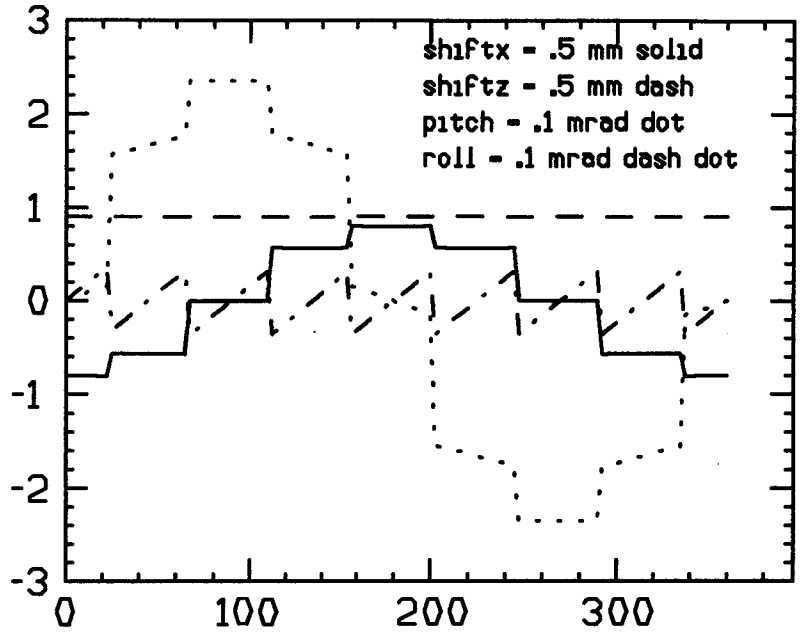

Fig 10-- Δ/σ vs φ Tor only Pt = 100 GeV

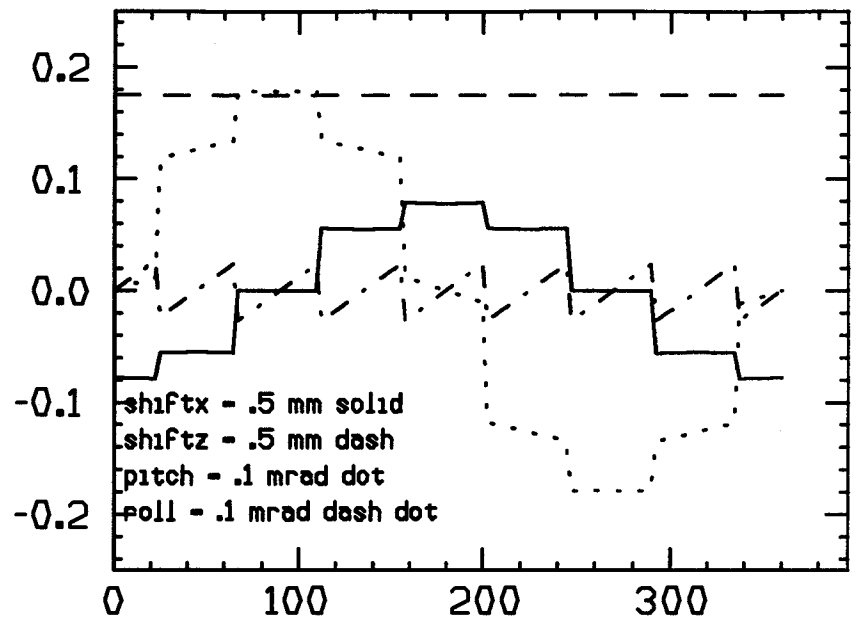

Fig 11--Δ/σ vrs φ φ-Trig Pt=100 GeV

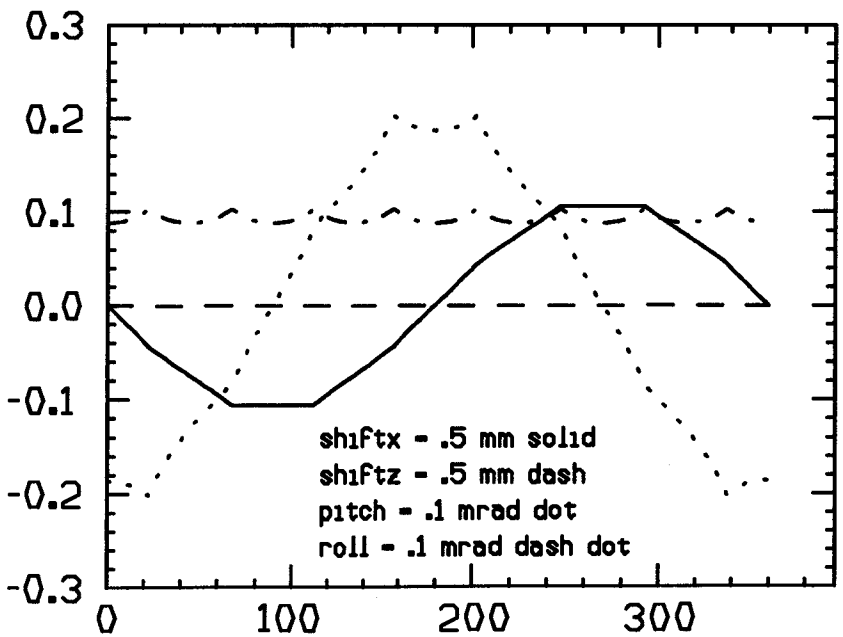
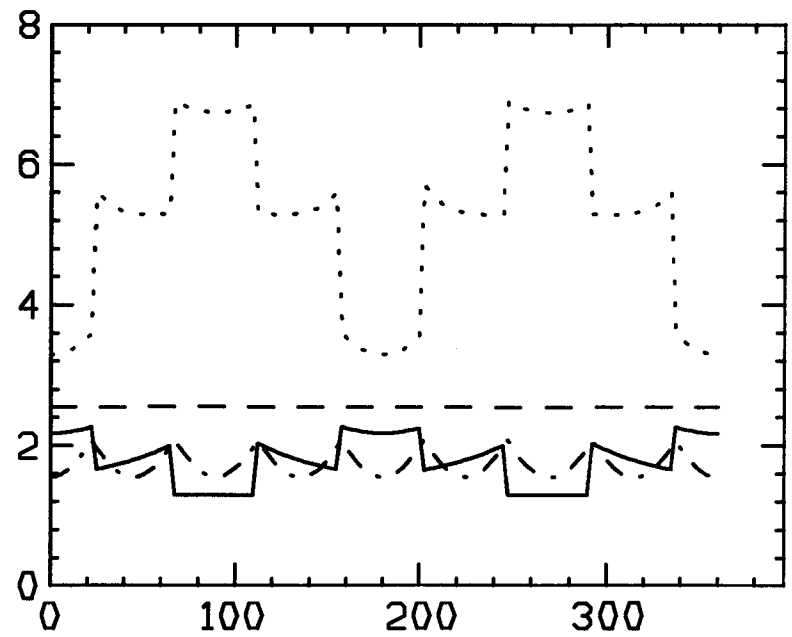
Fig 12 -- √ Δ χ vrs φ Pt = 2 TeV